Dyes and Pigments 223 (2024) 111919

Contents lists available at ScienceDirect

Dyes and Pigments

journal homepage: www.elsevier.com/locate/dyepig

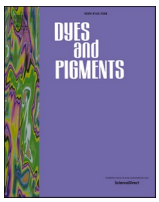

Chemical modification of 5-hydroxytryptophan photoinduced by endogenous sensitizers present in skin

Jesuán J. Farías [a], Paloma Lizondo-Aranda [b], Mariana P. Serrano [a], Andrés H. Thomas [a], Virginie Lhiaubet-Vallet [b,**], M. Laura Dántola [a,*]

[a] Instituto de Investigaciones Fisicoquímicas Teóricas y Aplicadas (INIFTA), Departamento de Química, Facultad de Ciencias Exactas, Universidad Nacional de La Plata, CCT La Plata-CONICET, Casilla de Correo 16, Sucursal 4, 1900, La Plata, Argentina

[b] Instituto Universitario Mixto de Tecnología Química, Universitat Politècnica de València - Consejo Superior de Investigaciones Científicas, Avenida de los Naranjos s/n, 46022, Valencia, Spain

ARTICLE INFO

Keywords:
5-Hydroxytryptophan
Aromatic pterins
UV-A radiation
Electron transfer reaction
Photodimerization
Tryptophan-4,5-dione

ABSTRACT

Damage caused to biological targets through sunlight photosensitized reaction is of paramount importance due to their potential effects on human health. In these processes, a chemical alteration of a biomolecule may occur as a result of the initial radiation absorption by another chemical species called photosensitizer. In this respect, pterins are endogenous photosensitizers able of inducing chemical modifications in DNA, proteins and lipids. These molecules are present in many living organisms and play different biological functions. In humans, aromatic pterins (Pt) accumulate in the depigmentation patches on the skin of patients suffering vitiligo. Interestingly, 5-hydroxytryptophan (5-OH-Trp), a common oxidation product of tryptophan acting as a potential endogenous antioxidant, is also present in the skin under oxidative stress conditions, such as those produced by vitiligo. However, the photochemical interaction between Pt and 5-OH-Trp has not been considered yet. With this background, the goal of the present work is to deepen the knowledge of the capability of Pt to photoinduce damage to 5-OH-Trp. By combining different analytical and spectroscopic techniques, we establish that 5-OH-Trp is damaged by Pt through a photosensitized type I process initiated by an electron transfer from the 5-OH-Trp to the Pt triplet excited state that yield the corresponding radical ions. In air-equilibrated aqueous solution four products were identified, two of which correspond to 5-OH-Trp dimers, while the others are a 5-OH-Trp trimer and a dione, in which the 5-OH-Trp has incorporated an oxygen atom. No consumption of Pt was observed in the presence of O_2. However, in the absence of O_2, further free-radical reactions lead to the reduction of the photosensitizer, and dimers and trimer were the only 5-OH-Trp-derived products detected. The biomedical implications of the generation of this kind of products, in proteins, are discussed.

1. Introduction

Vitiligo is an acquired skin depigmentation disorder that affects an estimated 1 % of the world population. It is characterized by the loss of constitutional pigmentation manifesting as white macules and patches, which extent is highly variable, ranging from focal to generalized pathologies. Patients with vitiligo accumulate millimolar levels of hydrogen peroxide (H_2O_2) in their epidermis. Upon reduction triggered by transition metal cations, or some organic compounds, H_2O_2 generates the highly reactive hydroxyl radical ($HO^{\bullet}$) that is able to oxidize many biomolecules [1,2]. The generation of this reactive oxygen species (ROS) leads to a severe epidermal stress, causing the deactivation of many enzymes and chemical modifications in proteins and peptides, by oxidation of different amino acid residues in their sequences [3]. It has been reported that in vitiligo, epidermal albumin levels are affected by oxidation, in which several amino acid residues are modified; for example, tryptophan (Trp) oxidation products like 5-hydroxytryptophan (5-OH-Trp), N-formylkynurenine (NFK) and kynurenine (KN) are found in the skin of sufferers [4].

Another clinical hallmark of vitiligo is the characteristic fluorescence of white skin patches when exposed to Wood's light (351 nm) examination [5]. This fluorescence has been attributed to the accumulation of

* Corresponding author. C.C. 16, Sucursal 4, (B1904DPI), La Plata, Argentina.
** Corresponding author. Instituto Universitario Mixto de Tecnología Química (UPV-CSIC), Avda de los Naranjos, s/n, 46022, Valencia, Spain.
E-mail addresses: lvirgini@itq.upv.es (V. Lhiaubet-Vallet), ldantola@inifta.unlp.edu.ar (M.L. Dántola).

https://doi.org/10.1016/j.dyepig.2023.111919
Received 5 August 2023; Received in revised form 29 November 2023; Accepted 21 December 2023
Available online 27 December 2023

aromatic pterins in the epidermis of affected individuals. Based on the epidermal overproduction of 5,6,7,8-tetrahydrobiopterins, the high levels of H_2O_2 and the lack of melanin in depigmented skin of these patients, it was plausible to assume that the oxidation and photo-oxidation of reduced pterins could occur, yielding aromatic pterins as products [6–11]. Pterins, a family of heterocyclic compounds derived from 2-aminopteridin-4(1*H*)-one, can exist in living systems in different redox states [12] and may be classified into three classes according to this property: fully oxidized (or aromatic) pterins, and dihydro and tetrahydro derivatives. The photochemistry and photophysics of pterins depend on their oxidation state [13]. Aromatic pterins are photochemically reactive in aqueous solutions and, under UV-A excitation (320–400 nm), they can fluoresce, undergo photooxidation to produce different products, and generate ROS such as singlet oxygen ($^1O_2$) and superoxide anion ($O_2^{\bullet-}$) [13,14]. These molecules can act as potential photosensitizers through both type I (electron transfer and/or hydrogen abstraction) and type II mechanisms (singlet oxygen) [15], the predominant one depends on a combination of many factors, such as quantum yields of $^1O_2$ production by the photosensitizer, reactivity of the substrate towards $^1O_2$, target molecule redox potential and presence of selective scavengers in the media [16,17].

Pterin (Ptr, Fig. 1), the parent and unsubstituted compound of oxidized pterins, under UV-A radiation is able to photoinduce damage in peptides and proteins present in the skin [18]. Studies performed with serum albumin (human and bovine) revealed that Ptr photosensitizes the oxidation and the oligomerization of albumin [19]. The photochemical reactions lead to the degradation of at least two amino acid residues: Trp and tyrosine (Tyr). In this process, albumin undergoes cross-linking, the bonds between the protein molecules are, at least in part, dimers of Tyr (Tyr_2). Trp is also consumed in the photosensitized process and NFK was identified as one of its oxidation products. These processes are purely dynamic and the main mechanism is initiated by electron transfer from the amino acid residues able to be oxidized by the triplet excited state of Ptr (^{3}Ptr*) [19].

The behaviour of aromatic pterins as endogenous photosensitizers is relevant to understand the harmful effects of radiation on skin, and is of particular interest in depigmentation disorders.With this background; the goal of the present work is to deepen the knowledge of the capability of pterins to photoinduce damage to molecules that are found in the skin. Taking this into account, 5-OH-Trp (Fig. 1) is target of choice as it has been found in the skin of vitiligo patients. Moreover, together with its derivatives, it has been suggested as potential endogenous antioxidant [20,21] having the ability to repair oxidized free-radical intermediates, such as indolyl of tryptophan, *via* one-electron transfer reaction. Based on the afore mentioned data, the simultaneous presence of Ptr and 5-OH-Trp in vitiligo patches together with the lack of pigmentation of these skin areas might boost their potential photochemical interaction, and result in photoproducts of biomedical relevance.

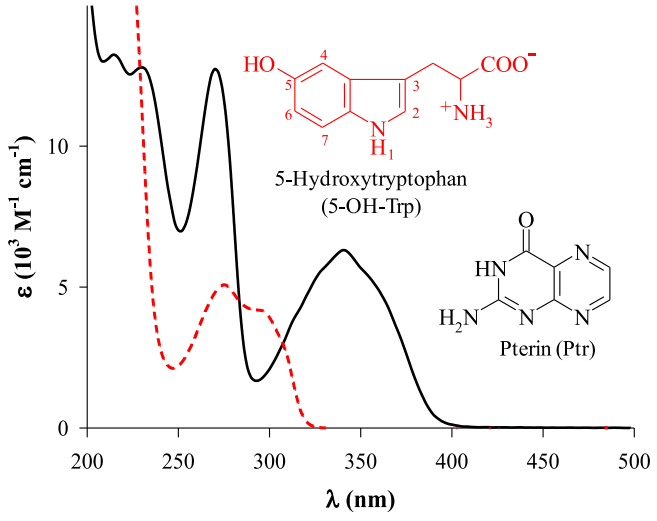

Fig. 1. Molecular structure and absorption spectra of pterin (Ptr) (black solid line) and 5-hydroxytryptophan (5-OH-Trp) (red dashed line) in air-equilibrated aqueous solutions at pH 5.5.

2. Material and methods

2.1. General

Chemicals. Pterin (Ptr) and 6-methylpterin (Mep)(purity >99 %, Schircks Laboratories, Switzerland), 5-Hydroxy-L-tryptophan (5-OH-Trp, purity >99 %), potassium iodide (KI), deuterated water (D_2O), superoxide dismutase (SOD) from bovine erythrocytes (lyophilized powder, ≥95 % biuret, ≥3000 units per mg of protein) and formic acid (HCOOH) were provided by Sigma-Aldrich and used without further purification. Experiments were carried out in aqueous solutions prepared using deionized water (specific electrical resistance of water was ~10 MΩ cm) further purified in a Milli Q Reagent Water System apparatus.

Measurements of pH. The pH measurements were performed using a pH-meter sensION + pH31 GLP combined with a pH electrode 5010T (Hach) or microelectrode XC161 (Radiometer Analytical). The pH of the aqueous solutions was adjusted by adding drops of HCl and NaOH solutions from a micropipette. The concentration of the acid and the base used for this purpose ranged from 0.1 to 2 M.

2.2. Steady-state irradiation

The continuous irradiation of the solutions containing photosensitizer (Ptr or Mep) and 5-OH-Trp were carried out in quartz cells at room temperature. Three different irradiation systems were employed: (I) the sample (1 mL) in quartz cell (1 cm optical pathlength) was irradiated with a Rayonet RPR 3500 lamp (Southern N.E.Ultraviolet Co.) with emission centered at 350 nm (bandwidth (full width at half-maximum) of ~20 nm, power 8 W), the distance between the lamp and the sample was 3 cm; (II) the sample (1 mL) (1 cm optical pathlength) was irradiated with two Rayonet RPR 3500 lamps the sample was at a distance of 3 mm from each lamp, (III) the sample (2 mL) was irradiated with Newport equipment composed by a Xenon Lamp (300 W), coupled, through a Mounting Kit (Model 74017), to a motorized monochromator UV-VIS (Oriel Cornerstone 130 1/8 m).

The experiments were performed in the presence and absence of dissolved O_2. Experiments with air-equilibrated solutions were carried out in open quartz cells without bubbling but stirring during irradiation time. Argon saturated solutions were obtained by bubbling for 20 min with this gas, previously water saturated (Linde, purity >99.998 %).

Aberchrome 540 (Aberchromics Ltd.) was used as an actinometer for the measurement of the incident photon flux density ($q_{n,p}^{0,V}$) at the excitation wavelength, which is the amount of incident photons per time interval ($q_{n,p}^{0}$) and divided by the volume of the sample [22]. The method for the determination of $q_{n,p}^{0,V}$ has been described in detail elsewhere [23]. The values of $q_{n,p}^{0,V}$ measured for the radiation sources were 4.0 (±0.4) x 10^{-6} E L^{-1} $s^{-1}$and 2.5 (±0.3) x 10^{-5} for irradiation setup I and II, respectively. Taking into account that the lamp emits quasi-monochromatic radiation, $q_{n,p}^{0,V}$ value was converted into the UV irradiance of the lamp (E_{UV}^{L}) with equation (1).

$$E_{UV}^{L} = q_{n,p}^{0,V} N_A h\nu \frac{V}{S} \quad (1)$$

where $N_A h\nu$ is the energy of a mol of photons emitted by the lamp and V

and S are, respectively, the volume and the area exposed to irradiation of the cell used. A value of 6.0 (±0.9) and 40 (±0.4) $W\ m^{-2}$ were obtained for E^{L}_{UV} when the sample were exposed to irradiation setup I and II, respectively.

2.3. Analysis of irradiated solution

UV/vis spectrophotometric analysis. Electronic absorption spectra were recorded on a Shimadzu UV-1800 spectrophotometer. Measurements were made using quartz cells of 0.4 or 1 cm optical pathlength. The absorption spectra of the solutions were recorded at regular intervals of irradiation time.

High-performance liquid chromatography (HPLC). A Prominence equipment from Shimadzu (solvent delivery module LC-20AT, on-line degasser DGU-20A5, communications bus module CBM-20, auto sampler SIL-20A HT, column oven CTO-10AS VP, photodiode array (PDA) detector SPD-M20A and fluorescence (FL) detector RF-20A) was employed for monitoring the photochemical processes. A Synergi Polar-RP column (ether-linked phenyl phase with polar endcapping, 150 × 4.6 mm, 4 μm, Phenomenex) was used for product separation and to analyze the progress of the photochemical processes. 100 % aqueous solution of formic acid (HCOOH, 25 mM, pH 5.0) was used as mobile phase.

In some cases, for further analysis, the products were isolated from HPLC runs (preparative HPLC), by collecting the mobile phase after passing through the PDA detector.

Detection and quantification of H_2O_2. For the determination of H_2O_2, a Cholesterol Kit (Wiener Laboratorios S.A.I.C.) was used. H_2O_2 was quantified after reaction with 4-aminophenazone and phenol [24,25]. Briefly, 500 μL of irradiated solution were added to 600 μL of reagent. The absorbance at 505 nm of the resulting mixture was measured after 30 min at room temperature, using the reagent as a blank. Aqueous H_2O_2 solutions prepared from commercial standards were employed for calibration.

Determination of O_2 concentration. The O_2 consumption during irradiation was measured with an O_2-selective electrode (Hansatech). The solutions and the electrode were placed in a closed glass cell of 2 mL.

Mass spectrometry analysis. Mass analyses were performed on two different systems. The first set-up is composed of Shimadzu modules: a DGU-405 degassing unit, a LC-40D xs solvent delivery module, a SCL-40 system controller, SIL-40C xs autosampler, a CTO-40C column oven, a SPD-M40 Photodiode array detector, and a Triple Quadrupole Mass Spectrometer LC 840 model. The same column (Sinergy Polar-RP column, 150 × 4.6 mm, 4 μm, Phenomenex) and eluting conditions (100 % aqueous solution of HCOOH) as described in the "High-performance liquid chromatography" section were used; injection volume was 20 μL. Analysis was performed using electrospray in positive mode with a capillary voltage of 4.5 kV. The following MS parameters were used in the analysis: Nebulizing Gas flow: 3 L min^{-1}, Drying Gas flow: 15 L min^{-1}, Interface temperature: 350 °C, Desolvation Line temperature: 250 °C, and Heating Block: 400 °C. The data were processed using Lab Solutions software.

The second system was used to determine the exact mass of the obtained photoproducts. It consists of a XevoQT of spectrometer (Waters coupled with an ultra-performance liquid chromatography system, with an autosampler conditioned at 10 °C. The separation was carried out on an UPLC with a Zorbax Eclipse Plus C18 (100 × 4.6 mm, 3.5 μm) column (ZC). The mobile phase was composed of 0.1 % HCOOH aqueous solution (component A) and 0.1 % HCOOH in acetonitrile (component B), and the flow rate was of 0.3 mL min^{-1}. The column was equilibrated with 100 % of A and a gradient was applied to reach A:B 5:95, v/v, over 22 min. The ESI source was operated in positive ionization mode with the capillary voltage at 1.6 kV, respectively. The source's temperature was set at 120 °C (positive mode), and the cone and desolvation gas flows were 10 and 800 L h^{-1}, respectively. All data were collected in centroid mode, and Leucine-enkephalin was used as the lock mass generating and $[M+H]^+$ ion (*m/z* 556.2771) at a concentration of 250 pg/mL and flow rate of 50 μL min^{-1} to ensure accuracy during the MS analysis.

Fluorescence spectroscopy. Fluorescence measurements were performed using a Single-Photon-Counting equipment FL3 TCSPC-SP (Horiba JobinYvon). The equipment has been previously described in detail [26].

Steady-state experiments. The sample solution in a quartz cell was irradiated with a 450 W Xenon source through an excitation monochromator. The fluorescence, after passing through an emission monochromator, was registered at 90° with respect to the incident beam using a room-temperature R928P detector. Corrected fluorescence spectra obtained by excitation at 340 nm were recorded between 380 and 550 nm, and total fluorescence intensities (I_F) were calculated by integration of the fluorescence band centered at *ca* 440 nm.

Time-resolved experiments. NanoLED source (maximum at 341 nm) was used for excitation. The emitted photons, after passing through the iHR320 monochromator, were detected at *ca* 440 nm by a TBX-04 detector connected to a TBX-PS power supply and counted by a FluoroHub-B module, controlled using the Data Station measurement control software application. The selected counting time window for the measurements reported in this study was 0–200 ns.

Laser Flash Photolysis. Laser flash photolysis (LFP) experiments were performed using a LP980 equipment. Briefly, pterins excitation was performed with the third harmonic at 355 nm of a Nd:YAG Surelite II-10 laser (6 ns *fwhm*, 10 mJ per pulse) of Continuum. The transient absorption spectra and decays of aqueous solutions of Ptr (~90 μM) and different 5-OH-Trp concentrations previously saturated by bubbling of Ar were recorded with the LP980 laser-flash photolysis apparatus (Edinburgh Instruments) linked to a 300 MHz Tektronik TDS 3012C digital oscilloscope for signal acquisition. The signal analysis was done with the Origin Pro 8.5 software from Origin Lab Corporation.

3. Results and discussion

3.1. Photosensitization of 5-hydroxytryptophan in the presence of oxygen

The first aim of this work was to find out if pterin (Ptr) was able to photoinduce the oxidation of 5-hydroxytryptophan (5-OH-Trp) in aqueous solutions upon UV-A irradiation. Therefore, air-equilibrated aqueous solutions containing Ptr and 5-OH-Trp were exposed to UV-A (350 nm) radiation for different periods of time (Irradiation setup I, Material and methods Section). Under these experimental conditions only Ptr was excited, as it can be inferred from the corresponding absorption spectra (Fig. 1). To better mimic the physiological conditions, experiments were performed using Ptr concentrations of the same order of magnitude as those found in human skin affected by vitiligo [27], and a pH of approximately 5.5, which is within the range of skin pH (varying between 4.5 and 5.8). It is noteworthy that under these conditions Ptr is present at more than 99 % in its acid form [13].The samples were analyzed by UV–vis spectrophotometry, HPLC and the concentration of H_2O_2 produced was measured (Material and methods Section).

The concentration profiles of Ptr and 5-OH-Trp, determined by HPLC, showed a decrease of the 5-OH-Trp concentration as a function of irradiation time, whereas the Ptr concentration did not change in the analyzed time-window (Fig. 2). Accordingly, four products called P1, P2, P3 and P4 at retention times (t_R) 3.5 min, 4.5 min, 7.5 min and 11.6 min, respectively, were detected by HPLC analysis of the irradiated solutions (Analysis of product Section) (Fig. S1, Supplementary material). H_2O_2 was found to be generated and its concentration increased as a function of irradiation time. However, its rate of production was lower than that corresponding to the initial rate of 5-OH-Trp consumption (Fig. 2). To discard a thermal reaction between H_2O_2 and 5-OH-Trp a control experiment was performed in which 5-OH-Trp was exposed to H_2O_2, at a concentration much higher than that generated during the

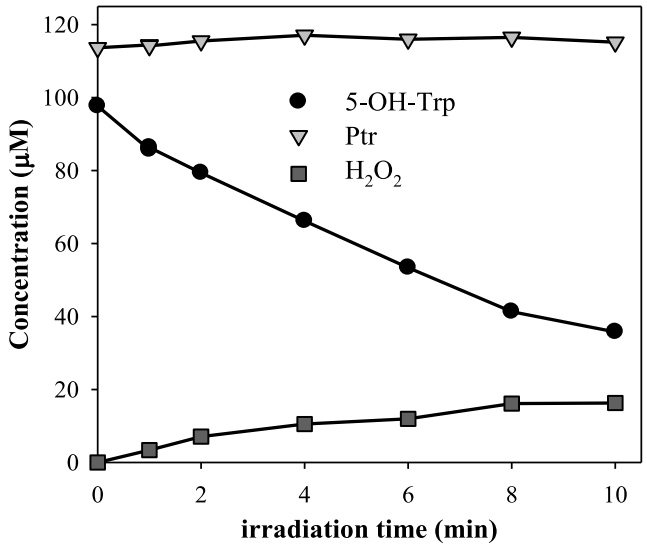

Fig. 2. Evolution of the 5-OH-Trp, Ptr and H_2O_2 concentrations in air-equilibrated aqueous solutions under UV-A irradiation as a function of time. $[5\text{-OH-Trp}]_0 = 98$ μM, $[\text{Ptr}]_0 = 110$ μM, irradiation system I, pH = 5.5 ± 0.1.

photochemical reaction, for a time longer than that used in the irradiation experiments. No consumption of 5-OH-Trp was observed (Fig. S2a, Supplementary material).

In experiments performed with a different optical geometry (Irradiation setup III, Material and methods Section), an O_2-selective electrode was used to monitor the decrease of the O_2 concentration upon irradiation of air-equilibrated solutions containing 5-OH-Trp (310 μM) and Ptr (110 μM) at pH 5.5 (Fig. 3). Control experiments in the absence of 5-OH-Trp, showed that the consumption of O_2 resulting from the photolysis of Ptr itself [28] was negligible in comparison with that observed in the presence of 5-OH-Trp (Fig. 3). No consumption of O_2 was observed when 5-OH-Trp was exposed to UV-A radiation in the absence of Ptr (Fig. 3). In several experiments, for determining the relationship between O_2 and 5-OH-Trp consumptions ($\Delta[O_2]/\Delta[5\text{-OH-Trp}]$), the solutions were analyzed by HPLC, before and after irradiation, to obtain the initial and final 5-OH-Trp concentrations, respectively. A value of *ca* 0.9 was obtained for $\Delta[O_2]/\Delta[5\text{-OH-Trp}]$ calculated for different irradiation times.

Thermal reactions between Ptr and 5-OH-Trp were discarded after control experiments performed by keeping solutions containing both compounds in the dark (Fig. S2b, Supplementary material). In another set of control experiments, 5-OH-Trp (107 μM, pH 5.5) solutions were irradiated in the absence of Ptr and no significant change of the 5-OH-Trp concentration was detected, thus discarding, as expected, direct effects of the radiation used on the 5-OH-Trp molecule (Fig. S2c, Supplementary material).Therefore, the results presented in this section clearly demonstrate that Ptr photosensitizes the oxidation of 5-OH-Trp under UV-A irradiation in air-equilibrated acid aqueous solutions.

In order to check the effect of the O_2 concentration, a new set of experiments were performed in O_2-saturated solutions at pH 5.5. Concentration profiles clearly showed that the rates of Ptr sensitized 5-OH-Trp disappearance was greater in air-equilibrated than in O_2-saturated solutions (Fig. 4).

It has been proved that O_2 quenches efficiently the triplet excited state of aromatic pterin derivatives (^{3}Pt*) [29]. The reduction in the rate of 5-OH-Trp consumption when O_2 concentration increases, strongly suggests that the ^{3}Pt* is involved in the photosensitization of 5-OH-Trp. To further investigate this, we have performed experiments in the presence of iodide (I^-). It has been previously demonstrated that I^- at micromolar concentrations is an efficient and selective quencher of ^{3}Pt* [30,31]. Therefore, photosensitization experiments were carried out in air-equilibrated aqueous solutions containing 5-OH-Trp (93 μM) and Ptr (115 μM) at pH 5.5 in the presence of KI (450 μM). The results revealed that, under these conditions, the rate of 5-OH-Trp consumption was slower than in the absence of I^- (Fig. 5a). Thus, considering that no quenching of the singlet excited state of Ptr (^{1}Ptr*) was previously observed at 450 μM of I^- concentration [31] the inhibition of the photosensitized degradation of 5-OH-Trp by I^- suggests the participation of the triplet excited state of Ptr (^{3}Ptr*).

Indeed, it is now well established that, on the one hand, ^{3}Ptr* gives rise to efficient singlet oxygen ($^1O_2$) formation upon UV-A irradiation ($\Phi_\Delta = 0.18 \pm 0.02$) [13], and on the other hand, this ROS is effectively quenched by 5-OH-Trp with a total quenching rate constant of $^1O_2$ of

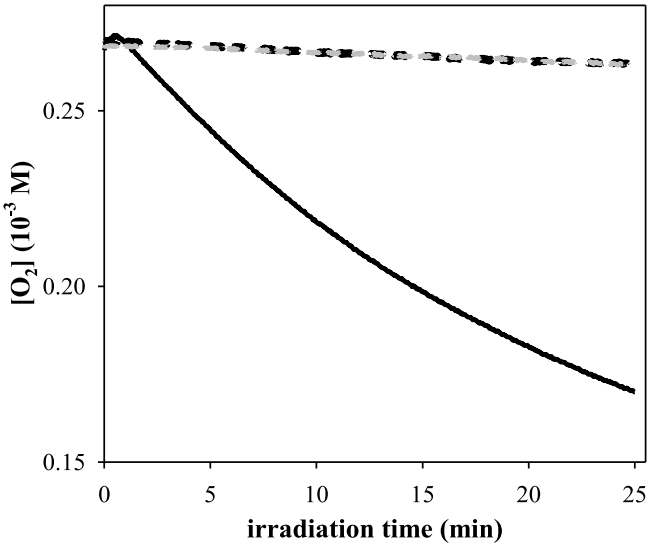

Fig. 3. Evolution of the O_2 concentration in irradiated solutions containing 5-OH-Trp and Ptr as a function of time (black solid line). Control experiment: photolysis of Ptr in the absence of 5-OH-Trp (black dashed line) and 5-OH-Trp in the absence of Ptr (gray dashed line). $[5\text{-OH-Trp}]_0 = 310$ μM, $[\text{Ptr}]_0 = 110$ μM, irradiation system III, pH = 5.5.

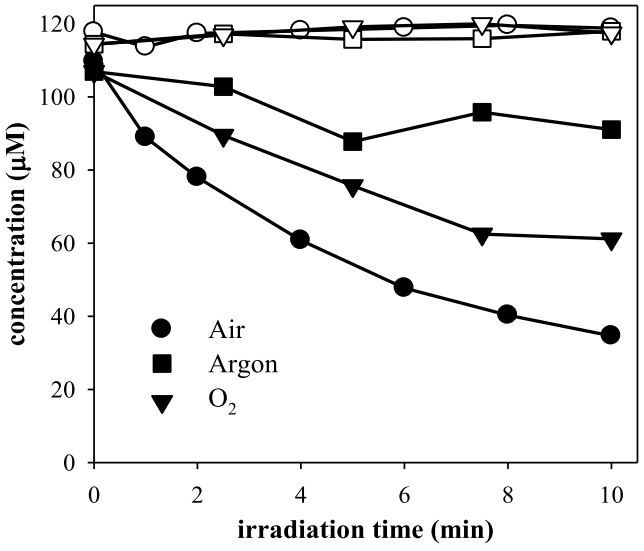

Fig. 4. Time evolution of 5-OH-Trp (filled symbols) and Ptr (empty symbols) concentration in air-equilibrated, O_2-saturated and O_2-free aqueous solution under UV-A irradiation. ($[5\text{-OH-Trp}]_0 = 107$ μM, $[\text{Ptr}]_0 = 115$ μM, irradiation system I, pH = 5.5). Errors on individual experimental points are ~4 μM.

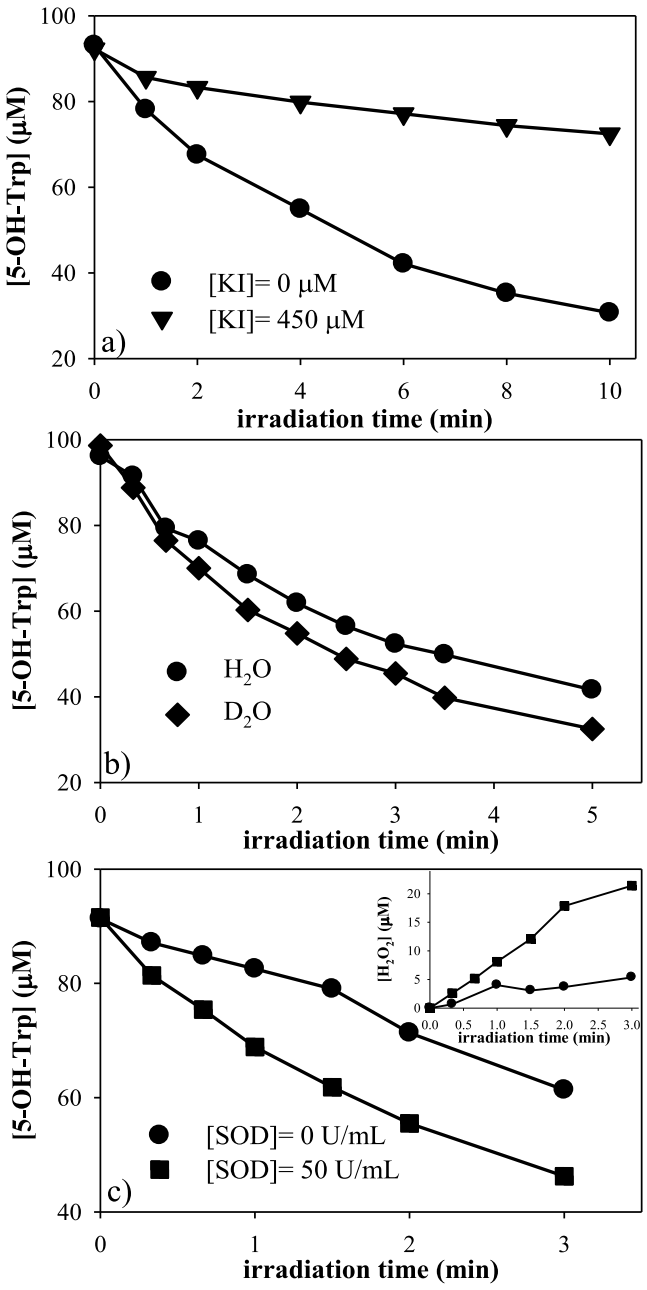

Fig. 5. Time evolution of 5-OH-Trp concentration during irradiation of air-equilibrated solution containing 5-OH-Trp and Ptr. a) in the absence and in the presence of KI ($[5\text{-OH-Trp}]_0 = 93$ μM, $[Ptr]_0 = 115$ μM; b) in D_2O and H_2O ($[5\text{-OH-Trp}]_0 = 100$ μM, $[Ptr]_0 = 120$ μM; c) in the absence and in the presence of SOD, inset: evolution of H_2O_2 concentration as a function of irradiation time ($[5\text{-OH-Trp}]_0 = 90$ μM, $[Ptr]_0 = 115$ μM). Irradiation system I, pH = 5.5.

1.26 (±0.4) x 10^8 $M^{-1}s^{-1}$ [32]. Therefore, it may be assumed that a type II mechanism is the origin of 5-OH-Trp photo-oxidation. To explore this point comparative photolysis experiments were performed in H_2O and D_2O. Given that the $^1O_2$ lifetime in D_2O is much longer than that in H_2O (*c.a.* 60 μs and 4 μs, respectively) [33] the rate of consumption of 5-OH-Trp should be about 15 times faster in the D_2O than in H_2O if the process takes place through a pure type II mechanism. Therefore, air-equilibrated solutions containing Ptr (120 μM) and 5-OH-Trp (100 μM) in H_2O and D_2O at pH/pD 5.5 were irradiated under identical conditions (Irradiation setup I, Material and methods Section). The rate of 5-OH-Trp consumption was barely higher in D_2O (Fig. 5b), but much lower than expected considering a pure type II mechanism. This might be interpreted as the competition between different processes as suggested by the significant difference between the rate constants of the reaction of amino acids with $^1O_2$ (Type II) [34] and with ^{3}Ptr*(Type I) [35].

Therefore, if the contribution of $^1O_2$ may be discarded or is negligible, a mechanism initiated by an electron transfer from the amino acid to the ^{3}Ptr* should be considered. The thermodynamic feasibility of this electron transfer between 5-OH-Trp and ^{3}Ptr* was determined using the Gibbs energy of photoinduced electron transfer Equation (2) [36]:

$$\Delta G = E^0(\text{5-OH-Trp}^{\bullet+}/\text{5-OH-Trp}) - E^0(\text{Ptr}/\text{Ptr}^{\bullet-}) - E_T(\text{Ptr}) \quad (2)$$

where E^0(5-OH-Trp$^{\bullet+}$/5-OH-Trp) is the reduction potential of 5-OH-Trp (*ca.* 0.64 V vs NHE) [32], E^0(Ptr/Ptr$^{\bullet-}$) is the reduction potential of Ptr (*ca.* −0.55 V vs NHE) and E_T(Ptr) is the triplet excited state energy of Ptr (*ca.* 2.52 eV) [37]. A value of ΔG = −1.34 eV was obtained, supporting that a photoinduced electron transfer between 5-OH-Trp and ^{3}Ptr* can spontaneously occur.

Moreover, it is well established that, in a typical type I process, ground state O_2 will readily quench an organic radical anion to produce the superoxide anion ($O_2^{\bullet-}$) [38,39]. The detected H_2O_2 (*vide supra*) can then be the product of the spontaneous disproportionation of $O_2^{\bullet-}$ in aqueous solution [40]. Therefore, we have investigated the participation of $O_2^{\bullet-}$ in the mechanism, by performing experiments at pH 5.5 in the presence of superoxide dismutase (SOD), an enzyme that catalyzes the conversion of $O_2^{\bullet-}$ into H_2O_2 and O_2 [41]. The data showed a significant increase in the rate of 5-OH-Trp consumption and H_2O_2 production when SOD was present in the solution (Fig. 5c). These results suggest that trapping of $O_2^{\bullet-}$ by SOD represents a pathway competing with a step that prevents the photoinduced oxidation of 5-OH-Trp (a more thorough explanation will be offered in the "Mechanism Overview Section").

3.2. Photosensitization of 5-hydroxytryptophan in the absence of oxygen

In experiments carried out in deoxygenated solutions (Irradiation setup I, Experimental Section), HPLC measurements showed a slight 5-OH-Trp consumption (Fig. 4), being P1, P2 and P3 the only photoproducts detected (Analysis products Section). No photosensitizer consumption was registered. To further investigate this point, new steady-state experiments in different conditions to those carried out in Fig. 4 were performed: higher 5-OH-Trp concentration (290 μM), higher irradiation intensity (Irradiation setup II, Experimental Section) and longer irradiation time. Under this experimental condition, considerable consumptions of 5-OH-Trp and Ptr were observed (Fig. S3, Supplementary material). These results suggest that 5-OH-Trp is photosensitized by Ptr in the absence of O_2 in a process slower than that observed in air-equilibrated solutions.

In previous reports we have demonstrated that aromatic pterins can undergo photoreduction in some particular cases, in which two conditions must be achieved: the absence of O_2, and the presence of a suitable electron donor [30,42]. In this reaction 7,8-dihydropterin derivatives are formed. The results described in the previous paragraph might be explained assuming a redox reaction where Ptr undergoes photoreduction. 7,8-Dihydropterin (H_2Ptr) is not commercially available and unstable, which makes it is difficult to confirm its formation in our reaction system. Therefore, we carried out additional experiments using 6-methylpterin (Mep). Mep is a compound with photochemical properties similar to Ptr [13], but its corresponding dihydroderivative, 6-methyl-7,8-dihydropterin (H_2Mep), is commercially available, rather stable and well characterized by chromatography [43]. The experiments were performed using the irradiation setup II (Material and methods Section), but at higher concentrations of 5-OH-Trp (300 μM) to favor the reaction. The HPLC-PDA, HPLC-MS and UPLC-HRMS analysis of irradiated solutions confirmed that H_2Mep is generated during irradiation, thus proving the photoreduction of the photosensitizer (Fig. S4 and Table S1,

Supplementary material). The concentration profiles showed that 5-OH-Trp and Mep, as in the case of Ptr, were also consumed, while H_2Mep concentration increased as a function of irradiation time (Fig. 6). A control experiment was performed in which 5-OH-Trp, under anaerobic condition, was irradiated in the absence of Mep. The HPLC analysis showed that 5-OH-Trp consumption is negligible in comparison with the consumption observed when Mep is present in the solution, confirming that the decreased in 5-OH-Trp concentration is due to a photosensitization process (Fig. S5a, Supplementary material). Another control experiment was performed in which Mep solution was exposed to UV-A radiation in the absence of 5-OH-Trp (Fig. S5b, Supplementary material). Although the Mep concentration decreased as a function of irradiation time, no H_2Mep formation was observed under these conditions. This result confirms that the photosensitizer is reduced only when 5-OH-Trp is present in the solution.

3.3. Deactivation of pterin excited state by 5-hydroxytryptophan

The study of the interaction of excited states of photosensitizers with biomolecules is useful to explain the mechanisms of photoinduced processes and to explore potential applications. Fluorescence quenching is a powerful tool for investigating the interaction of singlet excited states of fluorescent compounds with other molecules. Ptr in aqueous solution (pH = 6.0) under UV-A radiation forms ^{1}Ptr*, with a lifetime (τ_F) of 7.6 (±0.4) ns and a fluorescence quantum yield (Φ_F) of 0.33 (±0.01) [13]. Several studies have been performed on the quenching on ^{1}Ptr* by nucleotides and amino acids, finding that the efficiency of this process depends on the chemical structure of the quencher [35,44]. In the case of 5-OH-Trp, the deactivation of ^{1}Ptr* has not been previously studied. Therefore, fluorescence emission of the neutral form of Ptr (17 μM) was recorded in the presence and in the absence of 5-OH-Trp (0–4 mM), both in steady-state and time-resolved experiments (Material and methods Section). Emission spectra of Ptr were registered and a strong decrease in the fluorescence intensity (I_F) was observed with increasing 5-OH-Trp concentration (Fig. 7). In addition, the wavelength of the emission maximum remained unchanged (Fig. 7).

Furthermore, time-resolved studies were performed in the same experimental conditions; the emission was recorded at 440 nm. In the absence of 5-OH-Trp, a first-order kinetic was observed for the fluorescence decay of ^{1}Ptr*, with a τ_F value of 8.4 (±0.7) ns, which is in accordance, within the experimental error, with the previously published lifetime [13]. In the presence of different concentration of 5-OH-Trp, also first-order kinetics were observed for all the decays and the corresponding τ_F values decreased as a function of 5-OH-Trp concentration.

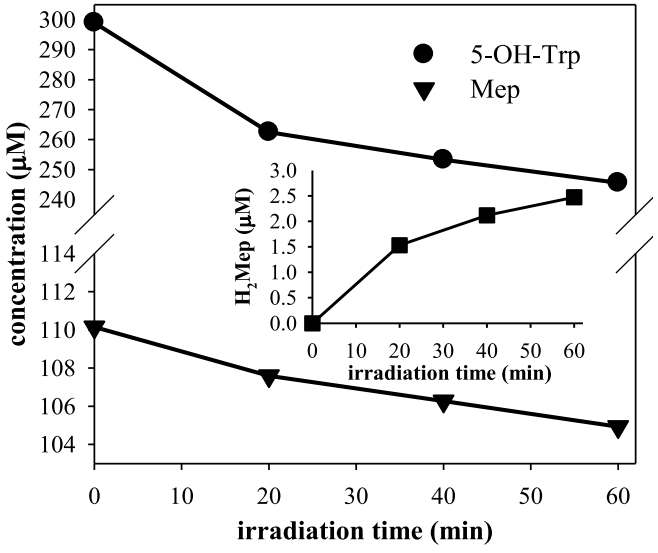

Fig. 6. Time evolutions of 5-OH-Trp, Mep and H_2Mep concentration, in O_2-free aqueous solution, under UV-A irradiation. ([5-OH-Trp]$_0$ = 300 μM, [Mep]$_0$ = 110 μM, irradiation system II, pH = 5.5).

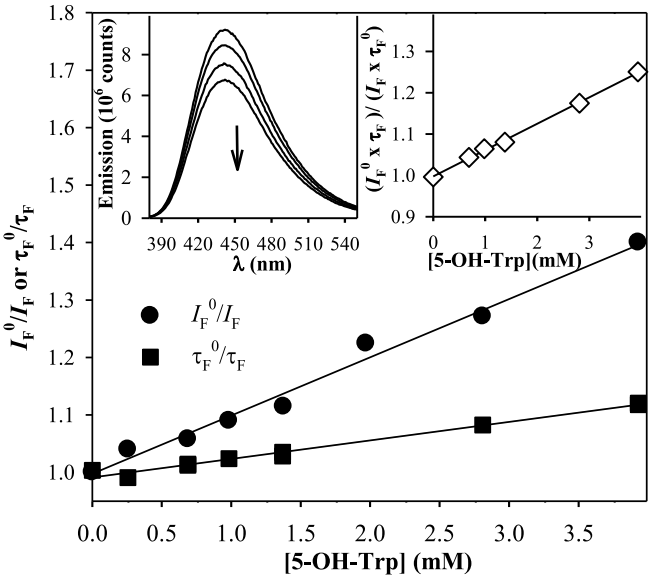

Fig. 7. Quenching of the fluorescence of Ptr by 5-OH-Trp. Stern-Volmer plots of the fluorescence intensities (I_F) and the fluorescence lifetimes (τ_F). λ_{exc} = 350 nm, λ_{em} = 440 nm, pH = 5.5. Left inset: Corrected fluorescence spectra registered at different 5-OH-Trp concentrations (0, 0.98 mM, 1.97 mM, 3.93 mM). Right inset: analysis of combined dynamic and static quenching: plot of $I_F^0\tau_F/I_F\tau_F^0$ *vs.* 5-OH-Trp concentration.

Fluorescence quenching can be evaluated by a Stern–Volmer analysis [45]. Considering the collision encounters between ^{1}Ptr* and 5-OH-Trp, purely dynamic quenching takes place and the results can be fitted with Equation (3):

$$\frac{I_F^0}{I_F}=\frac{\tau_F^0}{\tau_F}=1+K_D[5-OH-Trp]=1+k_q^F\tau_F^0[5-OH-Trp] \quad (3)$$

where I_F^0 and I_F are the integrated fluorescence intensities, and τ_F^0 and τ_F (s) the fluorescence lifetimes in the absence and in the presence of 5-OH-Trp, respectively, K_D (= $k_q^F\,\tau_F^0$) is the Stern–Volmer constant, with k_q^F as the bimolecular quenching rate constant of the ^{1}Ptr*. Therefore, if I_F^0/I_F *vs.* [5-OH-Trp] and τ_F^0/τ_F *vs.* [5-OH-Trp] are linear and coincident, a purely dynamic process can be assumed. However, when static quenching due to the formation of a 1:1 ground state complex between the fluorophore and the quencher occurs, the steady-state quenching is obtained from the contribution of both dynamic and static quenching components (Equation (4)),

$$\frac{I_F^0}{I_F}=(1+K_D[5-OH-Trp])(1+K_S[5-OH-Trp])=\frac{\tau_F^0}{\tau_F}(1+K_S[5-OH-Trp]) \quad (4)$$

where K_S is the equilibrium constant for complex formation. Since τ_F only depends on dynamic quenching, K_D and the corresponding k_q^F values are obtained by plotting τ_F^0/τ_F vs. [5-OH-Trp] (Equation (3)), while K_S can be easily obtained by rearranging Equation (4) as follows:

$$\frac{I_F^0}{I_F}\times\frac{\tau_F}{\tau_F^0}=1+K_S[5-OH-Trp] \quad (5)$$

The Stern-Volmer analysis of I_F and τ_F showed that the slope from the plots of $I_F^0/\ I_F$ *vs.* [5-OH-Trp] and $\tau_F^0/\ \tau_F$ *vs.* [5-OH-Trp] are not

coincident, indicating a deactivation of ^{1}Ptr* by a combination of dynamic and static processes. The k_q^F value obtained by plotting τ_F^0/τ_F vs. [5-OH-Trp] was 3.6 (±0.6) × 10^9 $M^{-1}s^{-1}$, which is in the range of diffusion-controlled limit. In addition, the plot of $I_F^0\tau_F/I_F\tau_F^0$ *vs.*5-OH-Trp concentration was perfectly linear (Fig. 7, inset), confirming the assumption of a combined dynamic and static (ground state complex) quenching mechanism, and the corresponding K_S value was calculated to be 64 (±9) M^{-1}. It indicates the association between Ptr ground state and 5-OH-Trp, which will be significant only at relatively high 5-OH-Trp concentrations.

In addition to the fluorescence emission, ^{1}Ptr*undergoes intersystem crossing to form short and a long-lived triplet excited states (^{3}Ptr*), corresponding to the lactim (0.36 (±0.08) μs) and lactam (3.9 (±0.7) μs) tautomers, respectively [29]. However, the ^{3}Ptr* lactam tautomer has been shown to be the only responsible for the photosensitized reactions using nucleotides, amino acids and proteins as targets [19,29,35]. Thus, interaction between ^{3}Ptr* and 5-OH-Trp was investigated by laser flash photolysis (LFP) experiments under anaerobic conditions (Material and methods Section). The lifetime for ^{3}Ptr* (τ_T) was recorded in the absence and in the presence of different 5-OH-Trp concentrations (Fig. 8). A growth was observed at 350 nm, which was selected as analysis wavelength. These signals obtained at different concentrations of 5-OH-Trp can be fitted with a mono-exponential growth function, and the Stern-Volmer analysis was carried out using Equation (6) (Fig. 8)

$$\frac{\tau_T^0}{\tau_T} = 1 + K_D^T[5-OH-Trp] = 1 + k_q^{5-OH-Trp}\tau_T^0[5-OH-Trp] \quad (6)$$

where τ_T^0 and τ_T are the triplet lifetimes (in s) in the absence (τ_T^0 = (5.4 ± 0.8) 10^{-6} s) and in the presence of 5-OH-Trp, respectively, and [5-OH-Trp] the concentration of the 5-OH-Trp in M. The Stern-Volmer plot obtained (Fig. 8) was linear and a value for $k_q^{5-OH-Trp}$ of (2.9 ± 0.4) 10^9 $M^{-1}s^{-1}$ was determined. Hence, these results confirm the efficient quenching of ^{3}Ptr* by 5-OH-Trp.

The results presented up to now strongly suggest that the photodegradation of 5-OH-Trp is initiated by an electron transfer from 5-OH-Trp to the ^{3}Ptr*. To explore this, we investigated the formation of the 5-indoloxyl-radical cation (5-OH-Trp$^{\bullet+}$) using LFP technique. S. Dad et al.

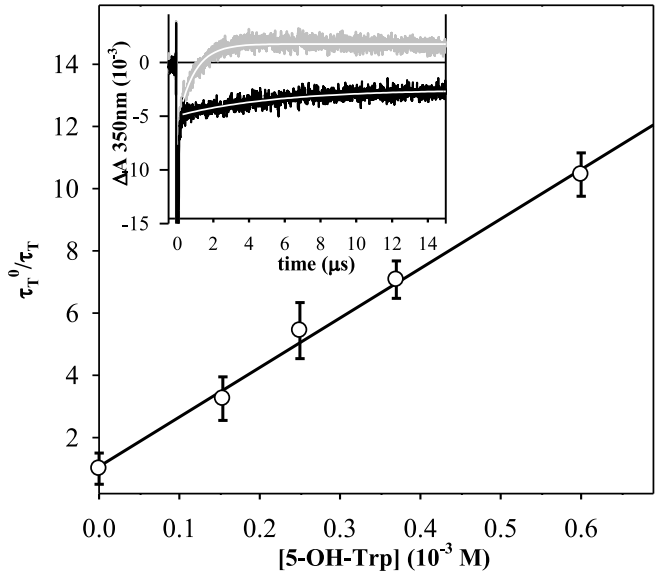

Fig. 8. Stern–Volmer plot of the quenching of the ^{3}Ptr* by 5-OH-Trp. τ_T values were calculated analyzing the transient absorbance ΔA *vs.* t; excitation wavelength 355 nm, analysis wavelength 350 nm, $[Ptr]_0$ = 90 μM. Inset: Time dependence of the absorbance at 350 nm at 0 (black line) and 0.25 mM (gray line) of 5-OH-Trp.

have characterized this radical by LFP, finding that the main feature of neutral 5-indoloxyl-radical (5-OH-Trp$^{\bullet}$) spectrum is the absorption maximun at 400–420 nm with around hundreds microseconds lifetime in water solvent (pK_a = − 0.7 ± 0.1) [32]. Transient absorption spectra obtained by laser-pulsed excitation of Ar-saturated solutions (pH 5.5) containing Ptr (90 μM) in the absence and in the presence of 5-OH-Trp (250 μM) were registered at different times after the laser pulse. In the absence of 5-OH-Trp the spectrum obtained showed a band with a maximum at around 430 nm and an absorption at wavelength longer than 500 nm, this spectrum satisfactorily correlated with the known spectral properties of ^{3}Ptr* [29]. When 5-OH-Trp is added to the Ptr solution, at a concentration in which the ^{3}Ptr* is completely deactivated, the spectrum obtained has an absorption band with a maximum between 400 and 420 nm (Fig. 9), which is characteristic of the neutral radical of 5-OH-Trp. Furthermore, an increase in absorbance is observed in the region around 350 nm, which corresponds to the formation of the radical. Consequently, the results confirm that the formation of the 5-OH-Trp radical proceeds by electron transfer from the 5-OH-Trp to ^{3}Ptr*.

3.4. Analysis of 5-hydroxytryptophan photoproducts

To complete the present study the analysis of products was carried out. For this, aqueous acid solutions containing 5-OH-Trp and Ptr (or Mep), at different O_2 concentrations, were analyzed by HPLC-PDA, fluorescence spectroscopy, HPLC-MS and UPLC-HRMS, before and after irradiation (Material and methods Section). As mentioned before, the HPLC-PDA analysis showed that, in air equilibrated aqueous solution, the photosensitization of 5-OH-Trp led to the formation of at least four products, called P1, P2, P3 and P4 (Fig. 10 and Fig. S1). Analysis of the chromatograms obtained at different wavelengths showed that the area of P1 and P2 peaks increased simultaneously (Fig. 10b and c), and were much larger than that corresponding to P4 (Fig. 10d). The spectra of the photoproducts P1 and P2 are quite similar with maxima at ca. 276 and 302 nm (Fig. 10a), while P4 showed the spectral features reported for tryptophan-4,5-dione (Fig. 10a) [46] with absorption bands at 250, 350 and 530 nm. Concerning the peak of P3, a poorly resolved spectrum with maxima at ca. 280 and 309 nm (Fig. S6, Supplementary Material) was extracted from the chromatograms; nevertheless, P3 intensity is too small to represent accurately the changes of its area as a function of irradiation time.

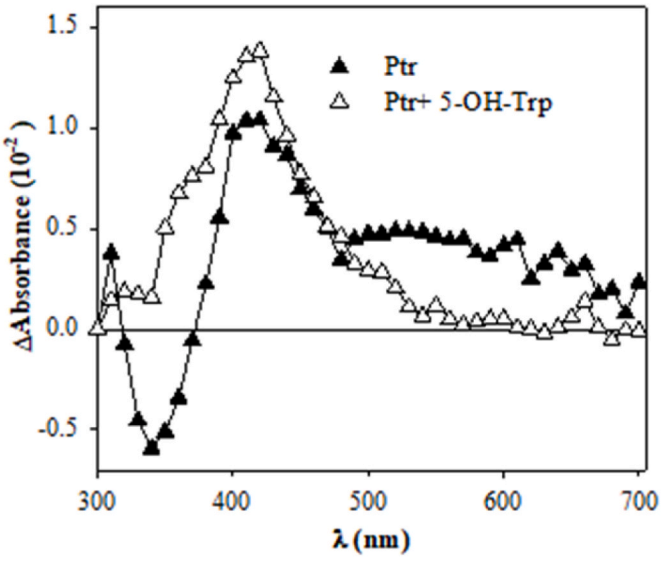

Fig. 9. Transient absorption spectra of Argon flushed aqueous solution of Ptr (90 μM) at pH 5 in the absence (black triangle, 1 μs after the laser pulse) or in the presence of 250 μM 5-OH-Trp (white triangle, 9 μs after the laser pulse).

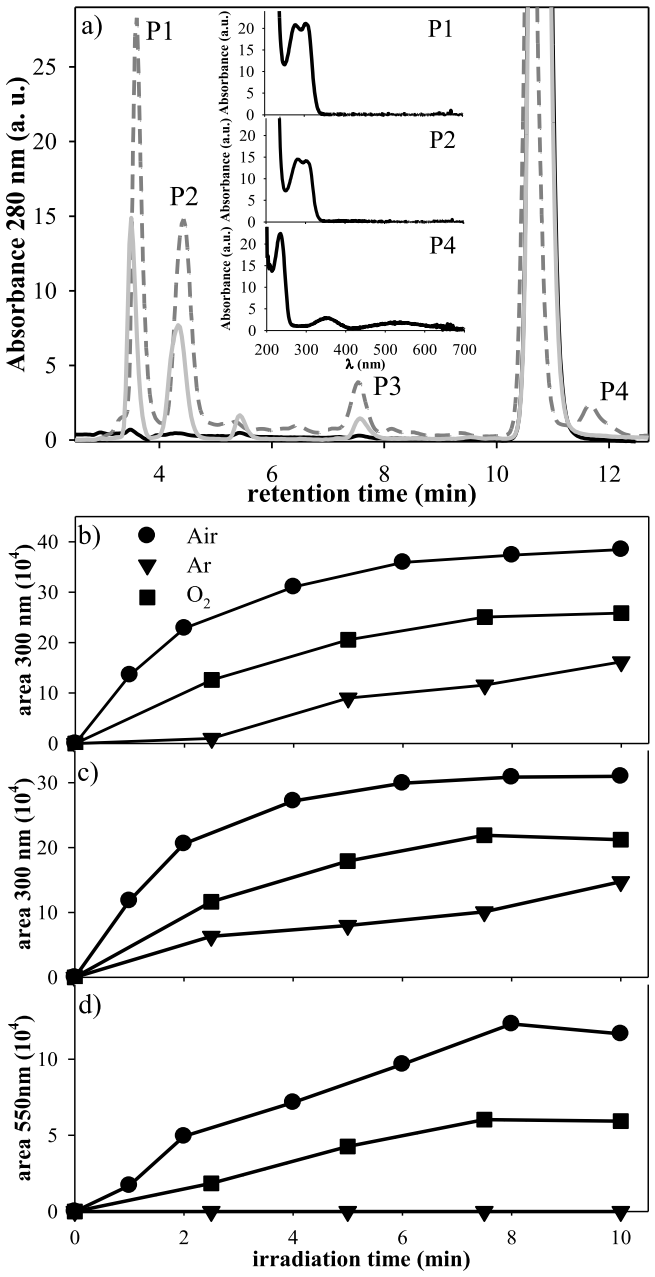

Fig. 10. a) HPLC-PDA chromatograms registered at 280 nm of a solution containing 5-OH-Trp and Ptr under aerobic (dashed gray line) and anaerobic conditions (solid gray line), before (solid black line) and after 10 min of irradiation. Inset: absorption spectrum of P1, P2 and P4. Time evolution of b) P1, c) P2 and d) P4 area in air-equilibrated, O_2-saturated and O_2-free aqueous solution under UV-A irradiation. ($[5\text{-OH-Trp}]_0 = 107$ μM, $[Ptr]_0 = 115$ μM, irradiation system I, pH = 5.5).

To gain insight on the structural characteristics of the products formed by the photosensitization of 5-OH-Trp, a qualitative analysis of these compounds was first carried out by HPLC coupled to mass spectrometry (HPLC-MS, Material and Methods Section) using the same column and conditions as for the HPLC-PDA analysis. Before irradiation chromatograms showed two peaks, and the mass spectrum recorded for these peaks exhibited the signal corresponding to the intact molecular ion of 5-OH-Trp and Ptr as $[M + H]^+$ species at *m/z* 221.1 (M: 5-OH-Trp) and 164.1 (M: Ptr), respectively (Table 1) (data not shown). After the irradiation, the mass spectrum at the retention times corresponding to

Table 1
Molecular formula, observed and calculated mass and mass error of 5-OH-Trp, Ptr and photoproducts detected in UPLC-HRMS spectra.

Compound	Elemental composition (M)		ESI $^+$ $(M + H)^+$		
		ion	calculated (*m/z*)	observed (*m/z*)	Error (ppm)
5-OH-Trp	$C_{11}H_{12}N_2O_3$	MH^+	221.0935	221.0926	4.1
Ptr	$C_6H_5N_5O$	MH^+	164.0572	164.0577	3.0
P1	$C_{22}H_{22}N_4O_6$	MH^+	439.1618	439.1620	0.5
P2	$C_{22}H_{22}N_4O_6$	MH^+	439.1618	439.1619	0.2
P3	$C_{33}H_{32}N_6O_9$	MH_2^{2+}	329.1194	329.1193	0.3
P4	$C_{11}H_{10}N_2O_4$	MH^+	235.0719	235.0725	3.4

P1, P2, P3 and P4 were recorded (Fig. S7, Supplementary Material). The mass spectra of P1 and P2, obtained in ESI^+ mode, showed *m/z* of 439.1 that is consistent with the formation of 5-OH-Trp dimers, $(5\text{-OH-Trp})_2$ with formula $[2M\text{-}2H + H]^+$, being M: 5-OH-Trp (Fig. S7, Supplementary Material). The mass spectrum recorded at the retention time of P4 showed a signal at *m/z* 235.1 (Fig. S7, Supplementary material), which agrees with its assignment as tryptophan-4,5-dione (Fig. 11). Finally, the mass spectrum registered at t_R corresponding to P3 showed a signal at *m/z* 329.1, which may be assigned to a (doubly charged) ion from 5-OH-Trp trimer $(5\text{-OH-Trp})_3$ (Fig. S7, Supplementary Material). This finding is interesting because it shows that the cross-linking of 5-OH-Trp does not stop in dimers, and that oligomers can be formed. Apart from these four main products, some additional products, with weak signals, were detected by HPLC-MS analysis. In particular, the *m/z* signals at 237 and 253 were registered, corresponding to products in which OH-Trp has incorporated one and two oxygen atoms, respectively. These results indicate that the products initially detected by HPLC-PDA analysis and confirmed by HPLC-MS analysis (P1, P2, P3 and P4) are not the only ones and, in contrast, other oxidation products, at lower concentrations, are also formed. This fact is expected taking into account the tryptophan photooxidation, which is very complex [1,47,48].

The molecular formulas of P1, P2, P3 and P4 were further confirmed by UPLC-HRMS, and the exact mass was obtained for the four photoproducts and initial compounds (Table 1). Thus, taking into account that P1 and P2 have the same molecular weight and absorption spectra, their structures should be different enough to produce a variation in the retention time in the chromatographic runs, which allows their separation and independent analysis. Indeed, numerous isomers have been proposed in the literature for Trp and 5-OH-Trp dimers [48,49] as they can arise from formation of a covalent link between the different atoms of the indolyl or phenyl moieties. Further structural information can be generally inferred from MS/MS analysis. The MS/MS spectra of P1 and P2 (Fig. S8, Supplementary material) revealed the typical fragmentation of the peptide side chain [50]. Interestingly, no signal corresponding to the fragmentation of the dimer into its original units was detected as proposed for indole-linked Trp dimers [51–53]. To get more information about the photophysical properties of P1 and P2, both products were isolated from the HPLC runs and the fluorescence spectra of P1 and P2 were recorded (Fig. S9, Supplementary material). Unlike what was reported for Trp dimers formed by covalent link between N1–C3′ or C3–C3′ of the indole rings [53] (see Fig. 1 for OH-Trp ring numeration), a significant bathochromic shift is observed in the emission spectrum of $(5\text{-OH-Trp})_2$ with respect to that of 5-OH-Trp [45]. This same behaviour was also observed in the dimerization of Tyr occurring between the two phenyl rings [54]. To the best our knowledge, no photochemical characterization of 5-OH-Trp photoproducts has been reported up to now. However, Humphries et al. achieved extensive studies on its electrochemical oxidation and described the full characterization of different $(5\text{-OH-Trp})_2$ and trimers $(5\text{-OH-Trp})_3$ after their isolation [46,55,56]. All compounds are derived from the coupling at the phenyl moieties, with the exception of an unstable dimer formed between position 6 and 3′ that finally yields a quinoline derivative. The *m/z* of this latter was not

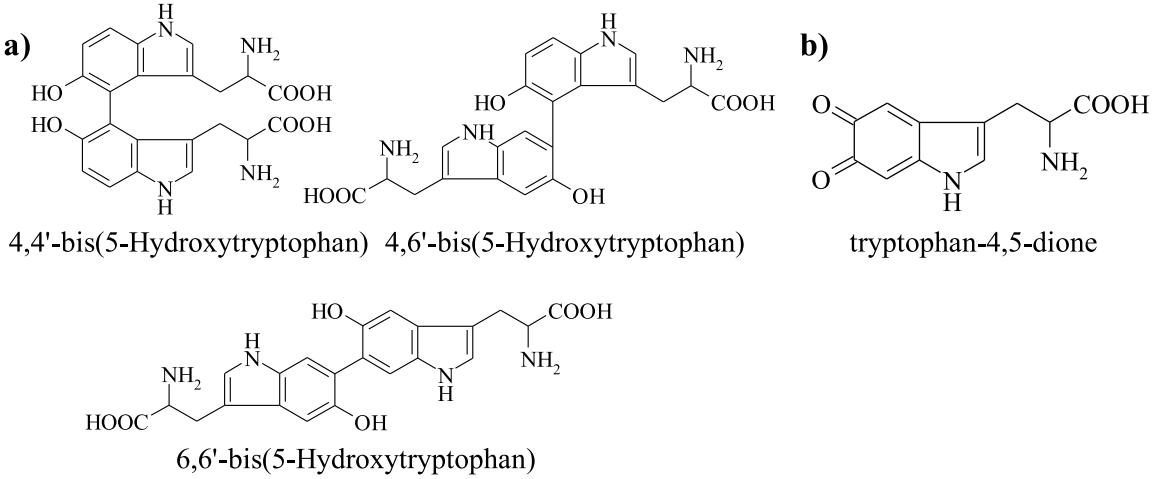

Fig. 11. Proposed molecular structure for the photoproducts a) P1, P2 and b) P4, detected in UPLC-HRMS analysis of acid aqueous solution of 5-OH-Trp exposed to UV-A radiation in the presence of aromatic pterin (Ptr or Mep).

detected in our analysis. Description of the UV–Vis absorption maxima of the different dimers, and trimers, provides interesting information. The absorption bands of C6–C6′, C4–C6′ and C4–C4′dimers suffer a bathochromic shift by respect to those of 5-OH-Trp, whereas, for dimers formed by covalent link between a carbon atom of the phenyl ring and the hydroxyl group at position 5, absorption maxima are similar to those of 5-OH-Trp. Similar observations were made for the trimers. Therefore, based on the UV absorption and fluorescence maxima together with the MS/MS spectra, we can hypothesize that P1 and P2 are dimers covalently linked through the phenyl ring (see Fig. 11), whereas P3 is a trimer formed from substitution at C6 and C4 of the central 5-OH-Trp. However, the lack of additional characterization (such as NMR spectra) does not allow an unambiguous structural assignment of those photoproducts.

The role of O_2 in the photogeneration of P1, P2 and P4 was analyzed. In the absence of O_2, P1 and P2 were the only products observed, being the amount of $(5\text{-OH-Trp})_2$ formed lower in anaerobic than in aerobic condition (Fig. 10b and c). This result is surprising because two 5-OH-Trp$^{\bullet}$ must combine to generate $(5\text{-OH-Trp})_2$. In the presence of O_2, others reactions compete with 5-OH-Trp$^{\bullet}$ dimerization to give oxygenated product (like P4), therefore the amount of $(5\text{-OH-Trp})_2$ formed should be higher in the absence of O_2. However, this was not the behaviour observed. The participation of O_2 in the mechanism of 5-OH-Trp dimerization will be discussed in the next section. Finally, as expected, P4 was not generated in the absence of O_2.

In overview, the results presented in this section showed that the photosensitization of 5-OH-Ptr by aromatic pterin under UV-A radiation induces the cross-linking and addition of oxygen of the 5-OH-Trp, which leads to formation of 5-OH-Trp dimer, trimer and tryptophan-4,5-dione, respectively. The generation of this kind of products may have harmful effects on proteins, since dimer can favor the oligomerization of this biomolecule, while the dione generates a new chomophore, and extend the active fraction of light able of being absorbed by the protein towards the visible range.

3.5. Mechanistic overview

Ptr photosensitizes the degradation of 5-OH-Trp in both aerobic and anaerobic conditions. Results of steady-state irradiations in D_2O and in the presence of SOD, LFP experiments and thermodynamic calculations demonstrated that, after the absorption of a photon by Ptr, the photosensitization process is initiated by the one-electron oxidation of 5-OH-Trp that takes place in the reaction between ^{3}Ptr* and the substrate (Reactions 1–3). As in the case of most nucleobases and aromatic amino acids, the radical cation of the substrate is in equilibrium with its neutral form (Reaction 4) [15]. Although O_2 does not participate in these steps, the rate of photodegradation of 5-OH-Trp strongly depends on the O_2 concentration (Fig. 4), being higher in air-equilibrated than in O_2-saturated solutions. This fact can be explained by the quenching of ^{3}Ptr* by O_2 (Reaction 5): at higher O_2 concentration, faster deactivation of ^{3}Ptr* and, consequently, slower reaction of ^{3}Ptr* with the substrate (Reaction 3). The $^1O_2$ generated in Reaction 5 does not contribute significantly to the oxidation of the substrate and, therefore, the lower amount of radicals formed in O_2-saturated solutions lead to an overall slower consumption of the substrate at high O_2 concentrations. Under anaerobic conditions the consumption of 5-OH-Trp is even slower than in O_2-saturated solutions. This can be interpreted considering the recombination of the radical ions in which the substrates are recovered (Reaction 6). This reaction is hindered when the radical anion of the photosensitizer ($Ptr^{\bullet-}$) reacts with O_2 (Reaction 7), which is in much higher concentration than the amino acid derived radical ($5\text{-OH-Trp}^{\bullet+}$/5-OH-Trp(-H)$^{\bullet}$). The superoxide anion ($O_2^{\bullet-}$), generated in this reaction (Reaction 7), then dismutates into H_2O_2 and O_2 (Reaction 8). Interestingly, in the presence of superoxide dismutase the rate of consumption of 5-OH-Trp is faster than in the absence of the enzyme. This result revealed that $O_2^{\bullet-}$ can also reduce 5-OH-Trp(-H)$^{\bullet}$ recovering the substrate (Reaction 9). The reaction scheme presented in this paragraph has previously been analyzed for the oxidation of other substrates photosensitized by Ptr and a more detailed discussion can be found in reference [17].

The analysis of photoproducts, described in the previous section, revealed the formation of, at least, two dimers through an oxygen-independent pathway and an oxygenated derivative, trypthophan-4,5-dione. In previous studies, carried out using Ptr as a photosensitizer, four types of situations have been described for the irradiation of an aqueous solution containing a biomolecule and Ptr under anaerobic conditions: i) no consumption of the substrate at all [29], ii) dimerization of the substrate [54], iii) formation of photoadducts [57,58], iv) photoreduction of the sensitizer [42]. It is difficult to predict which reaction will be the predominant one for a given biological target. Situation i) takes place when a reaction equivalent to Reaction 6 allows complete recover of the substrates, whereas situation ii) occurs when part of the substrate radicals are not reduced by Reaction 6 and can react to yield dimers (Reaction 10).

Molecular oxygen does not participate in any step of 5-OH-Trp dimers ($(5\text{-OH-Trp(-H)})_2$) formation, but, even so, their production is faster in air-equilibrated than in O_2-free solutions. This behavior has been observed and analyzed for the photosensitized formation of the Tyr

$$\mathrm{Ptr} \xrightarrow{h\upsilon} {}^{1}\mathrm{Ptr}^{*} \quad (1)$$

$${}^{1}\mathrm{Ptr}^{*} \longrightarrow {}^{3}\mathrm{Ptr}^{*} \quad (2)$$

$${}^{3}\mathrm{Ptr}^{*} + \text{5-OH-Trp} \longrightarrow \mathrm{Ptr}^{\bullet -} + \text{5-OH-Trp}^{\bullet +} \quad (3)$$

$$\text{5-OH-Trp}^{\bullet +} \rightleftharpoons \text{5-OH-Trp(-H)}^{\bullet} + \mathrm{H}^{+} \quad (4)$$

$${}^{3}\mathrm{Ptr}^{*} + \mathrm{O_2} \longrightarrow \mathrm{Ptr} + {}^{1}\mathrm{O_2} \quad (5)$$

$$\mathrm{Ptr}^{\bullet -} + \text{5-OH-Trp}^{\bullet +} \longrightarrow \mathrm{Ptr} + \text{5-OH-Trp} \quad (6)$$

$$\mathrm{Ptr}^{\bullet -} + \mathrm{O_2} \longrightarrow \mathrm{Ptr} + \mathrm{O_2}^{\bullet -} \quad (7)$$

$$2\ \mathrm{O_2}^{\bullet -} + 2\ \mathrm{H}^{+} \longrightarrow \mathrm{H_2O_2} + \mathrm{O_2} \quad (8)$$

$$\mathrm{O_2}^{\bullet -}(\mathrm{H}^{+}) + \text{5-OH-Trp(-H)}^{\bullet} \longrightarrow \text{5-OH-Trp} + \mathrm{O_2} \quad (9)$$

$$2\ \text{5-OH-Trp(-H)}^{\bullet} \longrightarrow (\text{5-OH-Trp})_2 \quad (10)$$

$$\text{5-OH-Trp}^{\bullet +}/\text{5-OH-Trp(-H)}^{\bullet} \xrightarrow{\mathrm{O_2}/\mathrm{H_2O}} \text{5-OH-Trp}_{(ox)} \quad (11)$$

dimer (Tyr_2) [59], and was tagged as "the oxygen paradox". In short, under anaerobic conditions two main pathways involving the substrate radicals compete: recombination of radicals (Reaction 6) and formation of dimers (Reaction 10); under aerobic conditions again three main pathways involving the substrate radicals compete: reaction between $O_2^{\bullet -}$ and 5-OH-Trp(-H)$^{\bullet}$ (Reaction 9), formation of dimers (Reaction 10) and oxygenation to yield the dione derivative, which, as a matter of fact, implicates several steps (Reaction 11). In the presence of O_2, reaction 7 is promoted, thus leading to a lower amount of Ptr$^{\bullet -}$ available to react with 5-OH-Trp$^{\bullet +}$/5-OH-Trp(-H)$^{\bullet}$ (Reaction 6). This in turn gives 5-OH-Trp(-H)$^{\bullet}$ a higher chance to dimerize. It is worth mentioning that in aerated solutions, although O_2 concentration is much higher than the substrate radical concentration, Reactions 10 and 11 take place at comparable rates. This fact reveals that the reactivity of 5-OH-Trp$^{\bullet +}$/5-OH-Trp(-H)$^{\bullet}$ towards O_2 is very low, which is not surprising since many radicals of biomolecules does not react fast efficiently with O_2 [15]. It is worth mentioning that "the oxygen paradox", by no means, can be considered a general behavior that is valid for any sensitizer and any biological target. In fact, it has been reported that the photodimerization of Trp with Rf is more efficient in anaerobic than in aerobic conditions [52]. A possible explanation for this behavior could be attributed to a higher efficiency of the recombination of the radical anion of the sensitizer and radical cation of the substrate (Reaction 6) when Ptr is used as sensitizer. The efficiency of this reaction for Ptr, has been demonstrated using different substrates as molecule target, in which no consumption of the substrate was observed when the photosensitization process is studied under anaerobic conditions [17].

4. Conclusions

The photosensitization of 5-hydroxytryptophan (5-OH-Trp), a common oxidation product of tryptophan (Trp), with the natural photosensitizer pterin (Ptr) and its methylated derivative 6-methylpterin (Mep) was studied, both in aqueous solutions at different O_2 concentrations. The process begins with an electron transfer from 5-OH-Trp to the triplet-excited state of the photosensitizer (Ptr or Mep), to yield the corresponding pair of radical ions. From this point two pathways are possible: i) an oxygen-independent pathway in which dimers are formed, ii) an oxygen-dependent pathway in which oxygenated products are generated. The formation of dimers takes places under both aerobic and anaerobic conditions; however, paradoxically it is faster in the presence of O_2.

Indeed, 5-OH-Trp and Ptr can be present simultaneously in the skin as the former is generated under oxidative stress and the latter is a natural photosensitizer that accumulates in patients suffering from skin depigmentations. Therefore, the photosensitization of 5-OH-Trp by Ptr is an interesting model to investigate the oxidative damage of human skin, triggered by electromagnetic radiation. In this sense, although the present work is not a study on human tissues, the results point out that the photoinduced oxidative damage does not stop at the first oxidation products. In contrast, further photosensitized chemical changes on oxidation products can lead to significant modifications in the composition of the system with different consequences. In this case, the formation of dimers might contribute to the photosensitized cross-linking of proteins, whereas the dione product is relevant because it absorbs in the visible region and, therefore, can suffer further photochemistry. This interesting point will be a subject of study in further research.

CRediT authorship contribution statement

Jesuán J. Farías: Data curation, Formal analysis, Investigation, Methodology. **Paloma Lizondo-Aranda:** Formal analysis, Investigation, Methodology, Data curation. **Mariana P. Serrano:** Formal analysis, Methodology, Data curation. **Andrés H. Thomas:** Conceptualization, Formal analysis, Funding acquisition, Methodology, Writing – review & editing, Data curation, Investigation. **Virginie Lhiaubet-Vallet:** Conceptualization, Formal analysis, Funding acquisition, Investigation, Methodology, Writing – review & editing, Data curation. **M. Laura Dántola:** Conceptualization, Data curation, Formal analysis, Funding acquisition, Investigation, Methodology, Supervision, Writing – original draft, Writing – review & editing, Project administration.

Declaration of competing interest

The authors declare that they have no known competing financial interests or personal relationships that could have appeared to influence the work reported in this paper.

Data availability

Data will be made available on request.

Acknowledgements

The present work was partially supported by Consejo Nacional de Investigaciones Científicas y Técnicas (CONICET-Grant P-UE 2017 22920170100100CO), Agencia de Promoción Científica y Tecnológica (ANPCyT-Grant PICT 2017–0925, PICT 2019–3416 and PICT 2020–03103), Universidad Nacional de La Plata (UNLP-Grant 11/X840). Also, financial support from CSIC (i-COOP, ref COOPB22038) and the Spanish (project PID2021-128348NB-I00 funded by MCIN/AEI/10.13039/501100011033/and "FEDER a way of making Europe", Sever Ochoa Center of Excellence Program CEX2021-001230-S) and regional (CIAICO/2021/061) governments is acknowledged. The authors deeply acknowledge Lic. Bruno Campanella (INIFTA, Argentina) for his valuable helps with the Laser Flash Photolysis measurements. J. J. F. thanks CONICET for doctoral research fellowship. M.L.D., M.P.S and A.H.T are research members of CONICET.

Appendix A. Supplementary data

Supplementary data to this article can be found online at https://doi.org/10.1016/j.dyepig.2023.111919.

References

[1] Davies MJ. The oxidative environment and protein damage. Biochim Biophys Acta 2005;1703:93–109.
[2] Cadet J, Wagner JR. Oxidatively generated base damage to cellular DNA by hydroxyl radical and one-electron oxidants: similarities and differences. Arch Biochem Biophys 2014;557:47–54.
[3] Schallreuter KU, Rübsam K, Gibbons NC, Maitland DJ, Chavan B, Zothner C, Rokos H, Wood JM. Methionine sulfoxide reductase A and B are deactivated by hydrogen peroxide (H2O2) in the epidermis of patients with vitiligo. J Invest Dermatol 2008;128:808–15.
[4] Rokos H, Wood JM, Hasse S, Schallreuter KU. Identification of epidermal L-tryptophan and its oxidation products by in vivo FT-Raman Spectroscopy further supports oxidative stress in patients with vitiligo. J Raman Spectrosc 2008;39:1214–8.
[5] Schallreuter KU, Wood JM, Pittelkow MR, Gütlich M, Lemke KR, Rödl W, Swanson NN, Hitzemann K, Ziegler I. Regulation of melanin biosynthesis in the human epidermis by tetrahydrobiopterin. Science 1994;263:1444–6.
[6] Schalleuter KU, Wood JM, Körner C, M Harle K, Schulz-Douglas V, R Werner E. Tetrahydrobiopterins functions as a UVB light switch for de novo melanogenesis. Biochim Biophys Acta 1998;1382:339–44.
[7] Armarego WLF, Randles D, Taguchi H. Peroxidase catalysed aerobic degradation of 5,6,7,8-tetrahydrobiopterin at physiological pH. Eur J Biochem 1983;135:393–403.
[8] Buglak AA, Telegina TA, Lyudnikova TA, Vechtomova YL, Kritsky MS. Photooxidation of tetrahydrobiopterin under UV irradiation: possible pathways and mechanisms. Photochem Photobiol 2014;90:1017–26.
[9] Buglak AA, Telegina TA, Vechtomova YL, Kritsky MS. Autoxidation and photooxidation of tetrahydrobiopterin: a theoretical study. Free Radic Res 2021;55:1–23.
[10] Vignoni M, Cabrerizo FM, Lorente C, Claparols C, Oliveros E, Thomas AH. Photochemistry of dihydrobiopterin in aqueous solution. Org Biomol Chem 2010;8:800–10.
[11] Dántola ML, Schuler TM, Denofrio MP, Vignoni M, Capparelli AL, Lorente C, Thomas AH. Reaction between 7,8-dihydropterins and hydrogen peroxide under physiological conditions. Tetrahedron 2008;64:8692–9.
[12] Buglak AA, Kapitonova MA, Vechtomova YL, Telegina TA. Insights into molecular structure of pterins suitable for biomedical applications. Int J Mol Sci 2022;23:15222.
[13] Lorente C, Thomas AH. Photophysics and photochemistry of pterins in aqueous solution. Acc Chem Res 2006;39:395–402.
[14] Oliveros E, Dántola ML, Vignoni M, Thomas AH, Lorente C. Production and quenching of reactive oxygen species by pterin derivatives, an intriguing class of biomolecules. Pure Appl Chem 2011;83:801–11.
[15] Baptista MS, Cadet J, Greer A, Thomas AH. Photosensitization reactions of biomolecules: definition, targets and mechanisms. Photochem Photobiol 2021;97:1456–83.
[16] Petroselli G, Dántola ML, Cabrerizo FM, Capparelli AL, Lorente C, Oliveros E, Thomas AH. Oxidation of 2′-deoxyguanosine 5′-monophosphate photoinduced by pterin: type I versus type II mechanism. J Am Chem Soc 2008;130:3001–11.
[17] Lorente C, Serrano MP, Vignoni M, Dántola ML, Thomas AH. A model to understand type I oxidations of biomolecules photosensitized by pterins. J. Photochem. Photobiol. 2021;7:100045.
[18] Dántola ML, Reid LO, Castaño C, Lorente C, Oliveros E, Thomas AH. Photosensitization of peptides and proteins by pterin derivatives. Pteridines 2017;28:105–14.
[19] Reid LO, Roman EA, Thomas AH, Dántola ML. Photooxidation of tryptophan and tyrosine residues in human serum albumin sensitized by pterin: a model for globular protein photodamage in skin. Biochemistry 2016;55:4777–86.
[20] Jovanovic SV, Simic MG. Tryptophan metabolites as antioxidants. Life Chem Rep 1985;3:124–30.
[21] Jovanovic SV, Simic MG. The DNA guanyl radical: kinetics and mechanisms of generation and repair. Biochim Biophys Acta 1989;1008:39–44.
[22] Braslavsky SE. Glossary of terms used in photochemistry, 3rd edition (IUPAC Recommendations 2006). Pure Appl Chem 2007;79:293–465.
[23] Kuhn HJ, Braslavsky SE, Schmidt R. Chemical actinometry (IUPAC technical report). Pure Appl Chem 2004;76:2105–46.
[24] Allain CC, Poon LS, Chan CSG, Richmond W, Fu PC. Enzymatic determination of total serum cholesterol. Clin Chem 1974;20:470–5.
[25] Flegg HM. An investigation of the determination of serum cholesterol by an enzymatic method. Ann Clin Biochem 1973;10:79–84.
[26] Serrano MP, Vignoni M, Dántola ML, Oliveros E, Lorente C, Thomas AH. Emission properties of dihydropterins in aqueous solutions. Phys Chem Chem Phys 2011;13:7419–25.
[27] Rokos H, Beazley WD, Schallreuter KU. Oxidative stress in vitiligo: photo-oxidation of pterins produces H_2O_2 and pterin-6-carboxylic acid. Biochem Biophys Res Commun 2002;292:805–11.
[28] Cabrerizo FM, Dántola ML, Thomas AH, Lorente C, Braun AM, Oliveros E, Capparelli AL. Photooxidation of pterin in aqueous solutions: biological and biomedical implications. Chem Biodivers 2004;1:1800–11.
[29] Serrano MP, Lorente C, Borsarelli CD, Thomas AH. Unraveling the degradation mechanism of purine nucleotides photosensitized by pterins: the role of charge-transfer steps. ChemPhysChem 2015;16:2244–52.
[30] Kritsky MS, Lyudnikova TA, Mironov EA, Moskaleva IV. The UV radiation-driven reduction of pterins in aqueous solution. J Photochem Photobiol B 1997;39:43–8.
[31] Denofrio MP, Ogilby PR, Thomas AH, Lorente C. Selective quenching of triplet excited states ofpteridines. Photochem Photobiol Sci 2014;13:1058–65.
[32] Dad S, Bisby RH, Clark IP, Parker AW. Identification and reactivity of the triplet excited state of 5-hydroxytryptophan. J PhotochemPhotobiol B 2005;78:245–51.
[33] Ogilby PR, Foote CS. Chemistry of singlet oxygen. 42. Effect of solvent, solvent isotopic substitution, and temperature on the lifetime of singlet molecular oxygen ($^1\Delta_g$). J Am Chem Soc 1983;105:3423–30.
[34] Michaeli A, Feitelson J. Reactivity of singlet oxygen toward amino acids and peptides. Photochem Photobiol 1994;59:284–9.
[35] Castaño C, Serrano MP, Lorente C, Borsarelli CD, Thomas AH. Quenching of the singlet and triplet excited states of pterin by amino acids. Photochem Photobiol 2019;95:220–6.
[36] Baptista MS, Cadet J, Greer A, Thomas AH. Practical aspects in the atudy of biological photosensitization including reaction mechanisms and product analyses: a do's and don'ts guide. Photochem Photobiol 2023;99:313–34.
[37] Song Q-H, Hwang KC. Direct observation for photophysical and photochemistry processes of folic acid in DMSO solution. J Photochem Photobiol A 2007;185:51–6.
[38] Hodgson EK, Fridovich I. The role of $O_2^{\bullet-}$ in the chemiluminescence of luminol. Photochem Photobiol 1973;18:451–5.
[39] Eriksen J, Foote CS, Parker TL. Photosensitized oxygenation of alkenes and sulfides via a non-singlet-oxygen mechanism. J Am Chem Soc 1977;99:6455–6.
[40] Bielski BHJ, Cabelli DE, Arudi RL, Ross AB. Reactivity of HO_2/O_2^- radicals in aqueous solution. J Phys Chem 1985;14:1041–100.
[41] Fridovich I. Superoxide radicals, superoxide dismutases and the aerobic lifestyle. Photochem Photobiol 1978;28:733–41.
[42] Dántola ML, Vignoni M, González C, Lorente C, Vicendo P, Oliveros E, Thomas AH. Electron-transfer processes induced by the triplet state of pterins inaqueous solutions. Free Radic Biol Med 2010;49:1014–22.
[43] Dántola ML, Schuler TM, Denofrio MP, Vignoni M, Capparelli AL, Lorente C, Thomas AH. Reaction between 7,8-dihydropterins and hydrogen peroxide under physiological conditions. Tetrahedron 2008;64:8692–9.
[44] Petroselli G, Dántola ML, Cabrerizo FM, Lorente C, Braun AM, Oliveros E, Thomas AH. Quenching of the fluorescence of aromatic pterins by deoxynucleotides. J Phys Chem A 2009;113:1794–9.
[45] Lakowicz JR. Principles of fluorescence spectroscopy. New York: Springer; 2006. p. 278–85.
[46] Humphries K, Dryhurst G. Electrochemical oxidation of 5 hydroxytryptophan in acid solution. J Pharmaceut Sci 1987;76(10):839–47.
[47] Pattison DI, Rahmanto AS, Davies MJ. Photo-oxidation of proteins. Photochem Photobiol Sci 2012;11:38–53.
[48] Sormacheva ED, Sherin PS, Tsentalovich YP. Dimerization and oxidation of tryptophan in UV-A photolysis sensitized by kynurenic acid. Free Radic Biol Med 2017;113:372–84.

[49] Paviani V, Junqueira de Melo P, Avakin A, Di Mascio P, Ronsein GE, Augusto O. Human cataractous lenses contain cross-links produced by crystalline-derived tryptophanyl and tyrosyl radicals. Free Radic Biol Med 2020;160:356–67.
[50] Zhang P, Chan W, Ang IL, Wei R, Lam MMT, Lei KMK, Poon TCW. Revisiting Fragmentation of protonated a-amino acid by high-resolution electrospray ionization tandem mass spectrometry with collision-induced dissociation. Sci Rep 2019;9(1):6453.
[51] Carroll L, Pattison DI, Davies JB, Anderson RF, Lopez Alarcon C, Davies MJ. Formation and detection of oxidant-generated tryptophan dimmers in peptides and proteins. Free Radic Biol Med 2017;113:132–42.
[52] Silva E, Barrias P, Fuentes-Lemus E, Tirapegui C, Aspee A, Carroll L, Davies MJ, López-Alarcón C. Riboflavin-induced Type 1 photo-oxidation of tryptophan using a high intensity 365 nm light emitting diode. Free Radic Biol Med 2019;131:133–43.
[53] Figueroa JD, Zarate AM, Fuentes-Lemus E, Davies MJ, Lopez-Alarcón C. Formation and characterization of crosslinks, including Tyr– Trp species, on one electron oxidation of free Tyr and Trp residues by carbonate radical anion. RSC Adv 2020; 10:25786–800.
[54] Reid LO, Castaño C, Dántola ML, Lhiaubet-Vallet V, Miranda MA, Marin ML, Thomas AH. A novel synthetic approach to tyrosine dimmers based on pterin photosensitization. Dyes Pigments 2017;147:67–74.
[55] Humphries K, Wrona MZ, Dryhurst G. Electrochemical and enzymatic oxidation of 5-hydroxytryptophan. J. Eletroanal. Chem. 1993;346(1–2):377–403.
[56] Humphries K, Dryhurst G. Biomimetic Electrochemistry: a study of the electrochemical and peroxidise-mediated oxidation of 5-hydroxytryptophan. J Electrochem Soc 1990;137:1144–9.
[57] Reid LO, Dántola ML, Petroselli G, Erra-Balsells R, Miranda MA, Lhiaubet-Vallet V, Thomas AH. Chemical modifications of globular proteins phototriggered by an endogenous photosensitizer. Chem Res Toxicol 2019;32:2250–9.
[58] Farías JJ, Lizondo-Aranda P, Thomas AH, Lhiaubet-Vallet V, Dántola ML. Pterin-lysine photoadduct: a potential candidate for photoallergy. Photochem Photobiol Sci 2022;21:1647–57.
[59] Dántola ML, Neyra Recky JR, Lorente C, Thomas AH. Photosensitized dimerization of tyrosine: the oxygen paradox. Photochem Photobiol 2022;98:687–95.